Dawn of the red and dead : stellar kinematics of massive quiescent galaxies out to z = 2

Sande, J. van de

1 Introduction

1.1 From galactic to extragalactic astronomy

On a dark clear night, one can observe a dim white strip of light crossing over the night sky from horizon to horizon: the Milky Way. Galileo Galilei, in the 17th century, was the first who pointed his telescope at this white cloud of light and discovered that it consisted of a huge number of stars. Inspired by the heliocentric model of our solar system from Nicolaus Copernicus, Immanuel Kant demonstrated in the mid-18th century, that this cloud in many ways resembled our solar system, but on a larger scale. In a similar way that the Planets are gravitationally bound to the Sun, he argued that the stars in the Milky Way could be gravitationally bound to each other, forming a disk-like structure. Thus the idea of a galaxy was born, although it was not fully understood. Kant furthermore proposed that our Galaxy, the Milky Way, might not be the only such cluster of stars, but that the faint elliptical nebulae in the sky could be individual *island universes*.

Towards the end of the eighteenth century Charles Messier (1781) compiled a catalog of the brightest 109 nebulae in the northern sky, of which the Andromeda Nebulae, or Messier 31, is the most famous example. William Herschel (1786) extended this catalog to nearly 5000 nebulae, but also made the distinction between unresolved nebulae and planetary nebulae. He was convinced that the unresolved nebulae were Kant's *island universes*, whereas the planetary nebulae resembled a single star with glowing gaseous material surrounding it. In later studies with more advanced telescopes the Earl of Rosse (William Parsons; 1845) revealed that even the unresolved nebulae consisted of two classes: elliptical and spiral. While there was no general consensus on the nature of these nebulae, there were two main rivaling ideas. Firstly, these nebulae could be part of our Milky Way as advocated by Harlow Shapley. Secondly, they could be extragalactic *island universes* similar to our Milky Way, a theory supported by Heber Curtis.

Spectroscopy on spiral nebulae provided valuable insight in favor of nebulae being extragalactic stellar systems. First, absorption features in the spectra resembled those of normal stars. Moreover, the overall spectral shape was consistent with the shape expected from a large population of stars (e.g., Slipher 1918). Secondly, the spectral lines of the nebulae were Doppler shifted, with inferred velocities many times larger than the stars in our Milky Way. Edwin Hubble 1922 finally settled the debate. By measuring the periods of the variable Cepheids stars in the outskirts of the Andromeda Nebula, he was able to estimate a distance of 300 kiloparsecs, which placed M31 far outside of our Milky Way. With this fundamental measurement, it was finally established that the spiral and elliptical nebulae were actually galaxies and that our Milky Way was not the only galaxy in the universe. Now, nearly a hundred years later, our knowledge of galaxies and galaxy formation has vastly expanded.

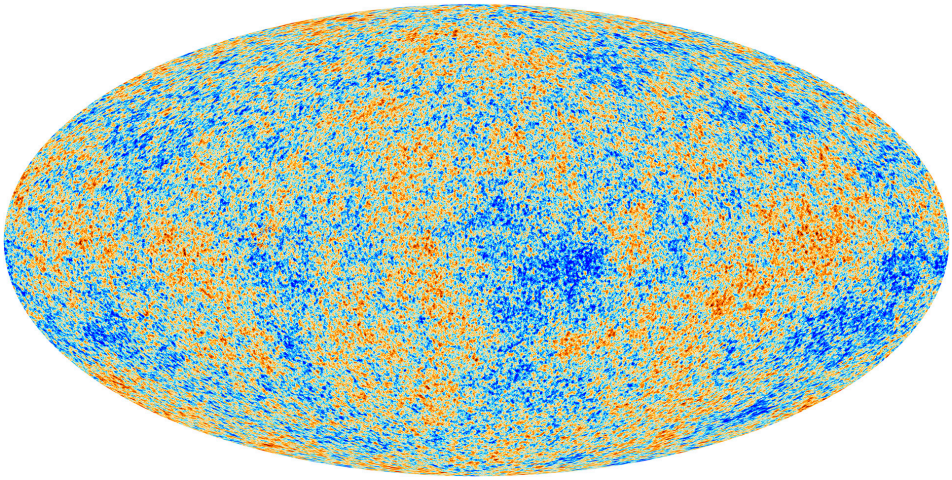

Figure 1.1: The anisotropies of the cosmic microwave background (CMB) radiation as observed by the Planck satellite. The CMB is a snapshot of the oldest light in our universe, from when it was only 380 000 years old. The color scale shows tiny temperature fluctuations on the order of 10^{-5} Kelvin, while the early-universe was still homogeneous and isotropic. These small fluctuations will grow into galaxies and clusters of galaxies. *Image: ESA & Planck Collaboration.*

1.2 Early universe & structure formation

The cosmic cosmic microwave background radiation (CMB; Gamow 1948; Hu & White 1996; Bennett et al. 2013) is the oldest light in the universe. According to the current theory, the CMB is leftover radiation from the Big Bang, which was emitted only 380,000 years after the beginning of the universe. After the Big Bang, 13.8 billion years ago, the universe started expanding and consequently cooling down, which enabled protons and electrons to form neutral atoms. From that moment on the universe became transparent as atoms could no longer absorb the thermal radiation. The first light that escaped is now still visible as a blackbody spectrum at a temperature of 2.72548 ± 0.00057 Kelvin, which is what is observed in the CMB radiation.

Due to the rapid early expansion, or cosmic inflation, the early universe was homogeneous and isotropic. On large scales the observed CMB is therefore very smooth; on small scales temperature fluctuations on the level of 10^{-5} exist (Figure 1.1). As our universe expanded and cooled over time, these small density perturbations grew through gravitational instabilities into the first galaxies. The smaller building blocks that form first then hierarchically merge into larger galaxies and clusters of galaxies. This is the foundation for the hierarchical structure formation model.

As the early universe was still extremely hot, normal baryonic matter was unable to cool and collapse. Cold dark matter enabled galaxy formation at this time, and is now considered to be the standard model or Lambda Cold Dark Matter (ΛCDM) model of structure formation. In this theory only $\sim 4\%$ of the energy density in the universe is made up of baryonic matter.

Gas, stars, dust are all made from baryonic matter. The remaining 96% of the universe's energy density consists of dark energy ($\sim$ 75%), and dark matter ($\sim$ 21%). While the nature of dark energy and dark matter remains unknown, clues for its existence are plentiful (e.g., Riess et al. 1998; Perlmutter et al. 1999; Clowe et al. 2006; Bradač et al. 2006; Bennett et al. 2013).

Within the gravitational collapsed perturbations, or dark matter haloes, the baryonic gas cools, and forms the first stars, giving rise to a visible galaxy. While the collapse of CDM is easily predicted from the theory of gravitation, the complex physics associated with star formation, stellar and nuclear feedback, and various other physical processes, is still not fully understood. Thus our theory on the formation of baryonic structure in the universe is still far from complete.

1.3 Local universe

While the extragalactic nature of many nebulae was only discovered in the 20th century, the large diversity in morphology was already identified long before (e.g., Herschel 1786; Earl of Rosse, 1845). Hubble (1936) was the first to construct a classification scheme, one that is still in use today. In Hubble's classification scheme, galaxies are classified by morphology into two separate classes: elliptical and spiral galaxies. Ellipticals vary in shape from round to elongated, with a smooth distribution of red-dominated light. Spirals consist of a red-central concentration, or bulge, with a surrounding disk with blue spiral structure. Roughly half of all spiral galaxies exhibit a prominent bar feature in their center which can extend out to the spiral arms. Based on his morphological classification, Hubble suggested that galaxies evolved from ellipticals into spirals. Hence, elliptical galaxies are commonly referred to as early-types, whereas spiral galaxies are known as late-type galaxies.

Galaxy morphology also correlates with other galaxy properties such as age, mass, and dynamics. In the local universe, ellipticals are predominantly massive, and consist of an old stellar population with very little ongoing star formation. Elliptical galaxies are supported by random motion of stars and this random motion is predominantly radial. These galaxies are commonly found in high-density environments such as groups and galaxy clusters. Spiral galaxies have lower masses and still show strong ongoing star formation, in particular in their disks. The motion of the stars in spiral galaxies are dominated by rotation. These galaxies are mostly observed in low-density environments.

Early-type galaxies furthermore obey a tight relationship between the half-light radius, the stellar velocity dispersion, and the average surface brightness. This structural scaling relation is known as the fundamental plane (FP; Faber & Jackson 1976; Djorgovski & Davis 1987; Dressler et al. 1987), and any of these three parameters can be estimated from the other two. Although spiral galaxies show a great diversity in many properties, they still obey a scaling relation between the intrinsic luminosity (proportional to the stellar mass) and rotational velocity. This relation is known as the Tully-Fisher relation (Tully & Fisher, 1977).

Given the fact that early-types are typically more massive, and contain old stellar populations, it is currently thought that galaxies evolve from disks to ellipticals, opposite as to Hubble proposed. Furthermore, it suggests that the process that is responsible for the morphological transition might also be responsible for quenching the star formation in galaxies. However, until the 21st century, extragalactic studies were based on relatively small numbers

of galaxies, which makes it harder to find the underlying mechanisms for the transition from spiral to elliptical.

The revolution came with observations from the Sloan Digital Sky Survey (SDSS; York et al. 2000), which provided the community with a large, well-understood statistical sample of galaxies. To date, this survey has provided optical photometry in five filterbands in combination with high-resolution spectra for over 800,000 galaxies in the northern-hemisphere. The photometry allowed for the determination of a galaxy's most basic properties: total luminosity, half-light or effective radius, and color gradient. The spectra yielded accurate redshifts, stellar spectral features, and stellar velocity dispersions. Combined, these measurements provided the framework for the most fundamental relations in galaxies such as the mass-size relation (Shen et al., 2003), the fundamental plane for elliptical galaxies (Bernardi et al., 2003), and also showed the environmental dependence of the relationships between stellar mass, structure, color, and star formation (Kauffmann et al. 2003, Blanton et al. 2005). One of the most important results from the SDSS is the clear bimodality of galaxies in the color-mass space (Figure 1.2). In this diagram early-type and late-type galaxies form two distinct classes. Early-type galaxies are found to have very red colors due to their old stellar populations, and lie on a tight relation in mass and $u - r$ color known as the red sequence. Late-type galaxies have a larger range in $u - r$ color, but are on average very blue due to the ongoing star formation. They have lower masses and reside in what is known as the blue cloud (Kauffmann et al. 2003, Blanton et al. 2005). Similarly to color, the bimodality is also present in other correlations with mass, such as the amplitude of the 4000 Å break (a stellar spectral feature from older stars that formed ionized metals), concentration of the light profile (Sérsic index), and specific star-formation rate.

The origin of this bimodality is perhaps the most fundamental question in extragalactic astronomy. One way to address this problem is by studying massive red-sequence galaxies, which are, according to the hierarchical merging theory, the final products of galaxy evolution. Detailed studies of massive elliptical galaxies in the local universe have proven to be invaluable, and tight scaling relations such as the fundamental plane, the red sequence, and their uniform old stellar populations provide a benchmark for galaxy evolution studies. Yet, observations of the present-day universe only provides an archaeological record of an early-type galaxy's past. In order to fully understand the formation and assembly of early-type galaxies, it is essential to observe galaxies at different stages in their evolution.

1.4 High-redshift observations

Due to the finite speed of light, an observation of a distant object offers us a view in the past. By observing galaxies at different distances, i.e., at different redshifts, we can study galaxies at earlier times, and thus witness the different epochs of galaxy evolution. Common techniques that are used at low redshift for determining morphology, effective radii, stellar masses and stellar population properties become, however, progressively harder at high redshift. Galaxies get fainter as their distance increases and require longer exposure times with large telescopes such as the Very Large Telescope (VLT) or Keck in order to obtain a similar signal-to-noise (S/N) as compared to low redshift. In particular, spectroscopy becomes increasingly difficult as the observed light is dispersed over a broad-wavelength range. Furthermore, at high red-

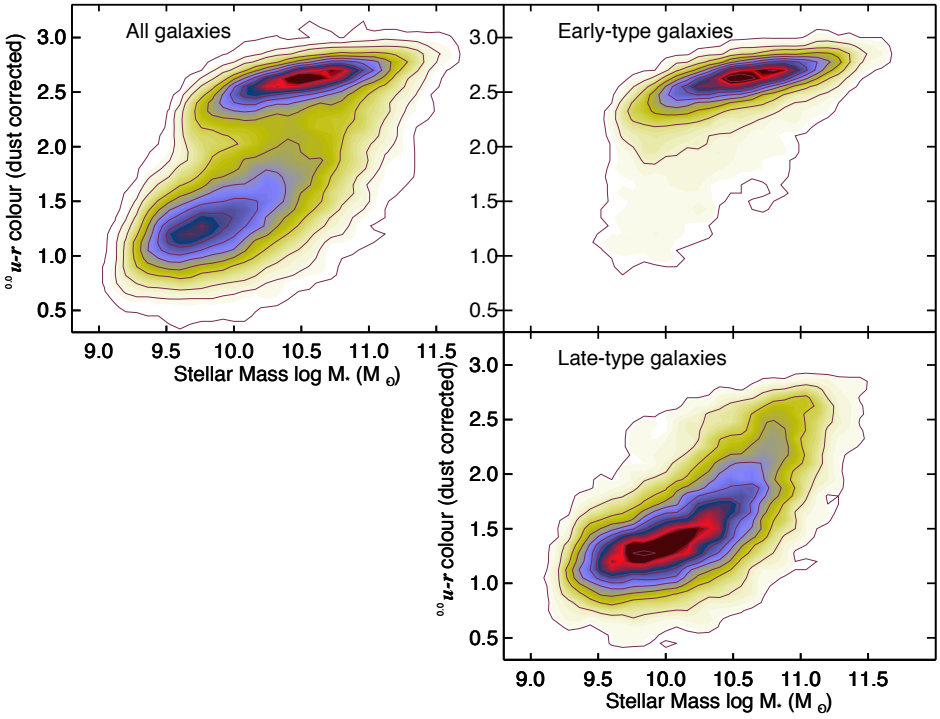

Figure 1.2: Bimodality in the local galaxy population, as shown in this rest-frame $u - r$ color vs. stellar mass diagram from Schawinski et al. (2014). The left panel shows all galaxies, whereas the right panel separates early-type (top) and late-type (bottom) galaxies. On average red-sequence galaxies are more massive than blue-cloud galaxies.

shift the rest-frame optical light is redshifted to the near-infrared (NIR) wavelengths where spectroscopy is more challenging as compared to optical wavelengths.

Yet, spectroscopy is required for determining accurate redshifts, which are essential for converting raw measurements into physical quantities such as size, total luminosity, and total stellar mass. For late-type galaxies with active star formation, a redshift is relatively easily obtained from bright emission lines, but for early-types with quiescent stellar populations, redshifts are measured from stellar absorption features in the faint stellar continuum.

A faster and cheaper technique for determining redshifts, using only photometry, is more commonly used, but this also comes with larger uncertainties. This technique is based on fitting a galaxy's observed photometric spectral energy distribution with templates from stellar population synthesis (SPS) models. Current SPS models provide an ensemble of templates for a large range in stellar population properties such as age and metallicity. A good template-fit to the observed data will provide a photometric redshift, stellar mass, and other important stellar population parameters. For obtaining statistical galaxy samples, large areas in the sky are observed in a multi-wavelength observing campaign using a set of carefully chosen filterbands, which range from the ultraviolet (UV) to the infrared (IR). This yields accurate photometry

and SEDs for thousands of galaxies at various redshifts.

While the overall shape of the SED can yield relatively accurate photometric redshift, some features in the SED provide even better results. For example, star-forming galaxies exhibit a sharp break around 912Å due to the Lyman-limit in the neutral hydrogen gas in the interstellar and intergalactic medium. At $z > 3$, this feature can be detected with optical broadband filters and is called the Lyman-break technique (Steidel et al. 1996a; 1996b). Early-type galaxies, with older stellar populations, have a spectral feature known as the Balmer/D4000-break, which is observable in the rest-frame optical. However at $z = 2$, the rest-frame optical light is redshifted into the NIR, where observations are technically more challenging as compared to optical wavelengths. Still, for both star-forming and quiescent galaxies, this SED fitting technique has proven to be extremely useful for obtaining photometric redshifts with an accuracy of 5% (Brammer et al., 2008).

Another difficult complication of studying galaxies out to $z = 1.5$ is that the angular size of an object decreases when observed at larger distances. This means that small galaxies at high redshift can no longer be resolved, which impedes morphological studies. Fortunately, due to the expansion and the shape of the universe, the minimum angular scale is reached around $z = 1.5$, after which galaxies grow in angular size again. While the diffraction limit of large telescopes is much smaller than the angular size of galaxies at high redshift, turbulence in the Earth's atmosphere degrades our images such that galaxies become unresolved from ground-based observatories. On good nights the full width at half maximum (FWHM) of the observed point spread function (PSF), or seeing, can be as good as 0.4-0.6 arcseconds ("), but is more typically around 0.″8-1.″0, while sizes of small massive galaxies are around 0.″1-0.″2. The Hubble Space Telescope (HST) has much better resolution, as it operates in space, outside of the Earth's atmosphere. In particular the Advanced Camera for Surveys (ACS) in the optical and Wide Field Camera 3 (WFC3) in the NIR are capable of reaching a FWHM of 0.″05, and 0.″12 respectively. Still, even with these state-of-the-art facilities such as HST, morphological measurements of galaxies at high redshift remain challenging.

1.5 Massive galaxies in the early universe

The first observations of galaxies at high redshift pictured a universe which was very different from the current universe. Using the Lyman-break technique, HST surveys mostly detected galaxies with very high star formation rates at $z > 2$ (e.g., Papovich et al. 2005). Furthermore, from HST-NICMOS imaging, these Lyman-break galaxies were found to be compact and often have irregular morphologies (e.g. Dickinson 2000). Ordinary spirals and ellipticals seemed to be largely absent at these redshifts. Yet, cosmological simulations suggested that the progenitors of elliptical galaxies formed at $z \sim 6$, after which they became very massive within a short amount of time ($M_* > 10^{11} M_\odot$) (Kereš et al. 2005; Khochfar & Silk 2006; De Lucia et al. 2006; Naab et al. 2007; Naab et al. 2009; Joung et al. 2009; Dekel et al. 2009; Kereš et al. 2009; Oser et al. 2010; Feldmann et al. 2010; Oser et al. 2012.)

However, due to observational challenges and selection effects early studies of the high-redshift universe were biased towards bright star-forming late-type galaxies, as quiescent early-type galaxies are faint in the rest-frame UV and thus not detected in optical surveys. Instead, early-type galaxies emit most of their flux in the rest-frame optical which corresponds

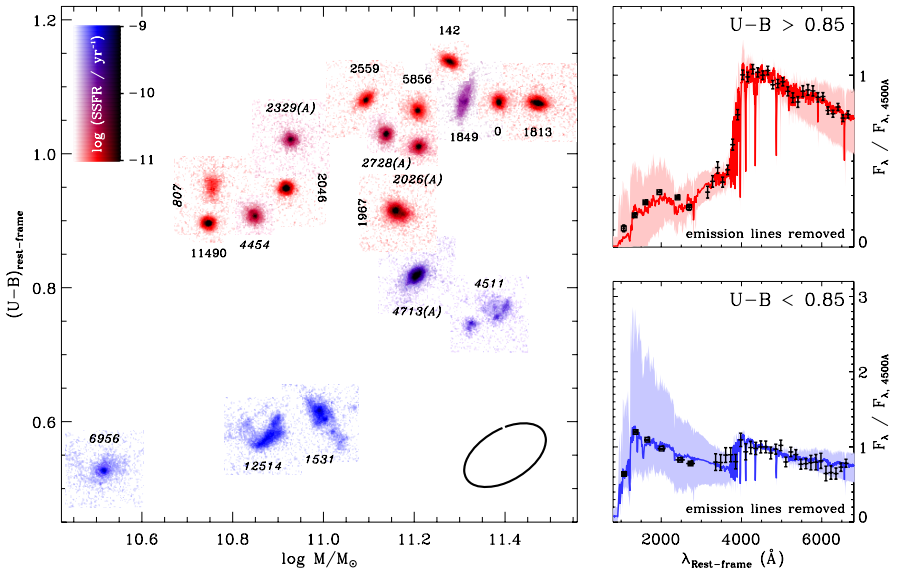

Figure 1.3: The Hubble sequence at $z \sim 2$ from Kriek et al. (2009b). Left: rest-frame $U - B$ color vs. stellar mass for massive galaxies with rest-frame optical spectroscopy. Different symbols are postage stamp images from HST-NICMOS-2, and the color coding represents the specific star-formation rate. A clear bimodality is visible, i.e., there is evidence of the red-sequence and blue-cloud as seen in Figure 1.2. Right: Stacked SEDs from GNIRS spectra and SPS models for red (top panel) and blue (bottom panel) galaxies, which shows that the two populations are truly distinct.

to the observed NIR for galaxies at $z = 2$.

With the advent of deep NIR surveys, which were designed to observe the rest-frame optical light of galaxies at high redshift (e.g., Labbé et al. 2003), distant red galaxies were indeed detected at $z = 2$ (e.g., Franx et al. 2003; van Dokkum & Stanford 2003, Labbé et al. 2005). NIR surveys typically selected galaxies in the NIR K-band, which means that they are no longer biased towards star-forming galaxies. Furthermore, as the rest-frame optical selection is a good proxy to mass selection, NIR surveys have become standard for obtaining a mass-complete sample of galaxies out to $z \sim 3$ (e.g., Wuyts et al. 2008; Williams et al. 2009; Whitaker et al. 2011; Muzzin et al. 2013a). With the wealth of information from broad to medium-band photometry and NIR spectrscopy, it has become clear that quiescent galaxies make up about half the galaxy population at high stellar masses (Daddi et al., 2005; Kriek et al., 2006; Muzzin et al., 2013b). Furthermore, the Hubble sequence might already exist at $z \sim 2$ (Figure 1.3, Kriek et al. 2008, 2009b; Szomoru et al. 2011). With increasingly deeper NIR surveys, massive quiescent galaxies have now been detected out to $z \sim 4$ (Straatman et al., 2014).

Even more surprising, these massive quiescent galaxies in the early-universe have been found to be extremely compact as compared to their present-day counterparts (Daddi et al., 2005; van der Wel et al., 2005; di Serego Alighieri et al., 2005; Trujillo et al., 2006; Longhetti

et al., 2007; Toft et al., 2007; Buitrago et al., 2008; van Dokkum et al., 2008; van der Wel et al., 2008; Cimatti et al., 2008; Franx et al., 2008; Damjanov et al., 2009; Cenarro & Trujillo, 2009; Bezanson et al., 2009; van Dokkum et al., 2010; Whitaker et al., 2012). At a fixed mass, massive quiescent galaxies at $z \sim 2$ have smaller effective radii by a factor 4-5 as compared to $z \sim 0$ galaxies. Almost none of these massive compact galaxies are observed in the local-universe (Trujillo et al., 2009; Taylor et al., 2010), which implies that massive galaxies must have undergone severe structural evolution. Thus, it is unlikely that early-type galaxies formed in an initial monolithic collapse, after which they passively evolved. If that were the case, their present-day counterparts would be too small and too red (van Dokkum et al., 2008; Kriek et al., 2008; Bezanson et al., 2009; Ferré-Mateu et al., 2012). Instead, these $z \sim 2$ galaxies are likely the cores of present-day ellipticals that have grown in an inside-out fashion, mainly by adding stellar mass to the outer parts over time (Hopkins et al., 2009b; van Dokkum et al., 2010; Szomoru et al., 2012; Saracco et al., 2012).

The dominant physical mechanism for this structural evolution is still a subject of ongoing debate. In the hierarchical structure formation theory, merging is considered a natural process and is expected to play an important role in the structural and morphological evolution of massive galaxies (e.g.Kauffmann et al., 1996; Kauffmann, 1996; De Lucia et al., 2006; Khochfar & Silk, 2006; De Lucia & Blaizot, 2007; Guo & White, 2008; Kormendy et al., 2009; Hopkins et al., 2010). Observations of early-type galaxies out to high redshifts indeed show evidence of mergers taking place (van Dokkum, 2005; Tran et al., 2005; Bell et al., 2006a,b; Lotz et al., 2008; Jogee et al., 2009; Newman et al., 2012; Man et al., 2012). However, size growth due to major mergers seems to be unlikely, as there are not enough major mergers that can account for the large size evolution, and the predicted increase in size is insufficient in bringing $z \sim 2$ galaxies closer to the $z \sim 0$ mass-size relation (e.g., Naab et al. 2007; Nipoti et al. 2009; Bundy et al. 2009; de Ravel et al. 2009; Bluck et al. 2009). Minor mergers, however, are expected to occur more frequently in the lifetime of a massive galaxy, and could offer a solution to this problem. With only a few assumptions from the Virial theorem, Cole et al. (2000), Naab et al. (2009), and Bezanson et al. (2009) show that minor mergers are very efficient in increasing the size of a galaxy, without a significant increase in mass. Simulations of merging galaxies also predict that minor-mergers are likely the dominant process for increasing galaxy sizes (Hopkins et al. 2009; Oser et al. 2012; Hilz et al. 2013; Bédorf & Portegies Zwart 2013). From observations, several studies suggest that minor mergers could be responsible for the size growth at $0 < z < 1$, while at higher redshift there might not be enough minor mergers to explain the observed growth (Oogi & Habe, 2012; Nipoti et al., 2012; Cimatti et al., 2012; Newman et al., 2012).

1.6 Current issues

As with any new major discovery, there has been a debate about the reality of this structural evolution. Errors in the size and mass estimates are possible explanations for the compactness of massive high-redshift galaxies. Initial concerns that the size is being underestimated due to an envelope of low-surface brightness light, have been addressed with deep HST-WFC3 imaging. Szomoru et al. (2010; 2012) measure the surface brightness profiles for a sample of quiescent galaxies at $1.5 < z < 2.5$, using a method that properly measures low surface

brightness flux at large radii. They find that quiescent galaxies have effective radii that are a factor ~ 4 smaller than those of low-redshift quiescent galaxies of similar mass, and have no excess flux at large radii. Subsequent work by van der Wel et al. (2014; and references therein) confirms these results. Other methods, such as stacking, also show that sizes increase over time. (e.g., van der Wel et al. 2008; Cassata et al. 2010; van Dokkum et al. 2008, 2010). The light could also be more concentrated due to the presence of active galactic nuclei (AGNs) in these galaxies. However, spectra of subsamples of these galaxies show that the light is dominated by evolved stellar populations, not AGNs (Kriek et al. 2006, 2009; Onodera et al. 2012)

Color gradients in galaxies can also lead to large discrepancies when comparing sizes at different redshifts. A small amount of recent star formation in the center of a galaxy can create a bias toward small sizes, as the light from the young hot blue stars out-shines the older population. This issue becomes less of a problem when looking at the redmost possible wavelengths, but this becomes increasingly harder at $z > 2$ where the rest-frame optical is redshifted to the NIR wavelengths. Szomoru et al. (2013) accurately measure the surface brightness in several filterbands and find that the overwhelming majority of galaxies has negative radial color gradients, such that the cores of galaxies are redder than the outskirts. Furthermore, they show that stellar half-mass radii from the mass profiles are on average $\sim 25\%$ smaller than rest-frame g-band half-light radii. Thus, these results show that the small sizes at high redshift are not due to systematic uncertainties.

The question of whether stellar masses are accurate out to $z \sim 2$ remains, however, a serious concern. An overestimate in stellar mass would bring the galaxies closer to the $z \sim 0$ mass-size relation. To date, basically all (stellar) masses have been derived by fitting SEDs. This method suffers from many systematic uncertainties in SPS models, metallicity, star formation history (SFH), and the stellar initial mass function (IMF) (e.g., Maraston et al. 2006; Muzzin et al. 2009; Conroy et al. 2009).

SPS models are now widely used for fitting the SEDs of galaxies, and can be used effectively to derive many physical properties, such as redshift, stellar mass, star formation rate, dust content, and metallicity. Generally, these models construct simple stellar populations (SSPs) from basic inputs: stellar evolution theory in the form of stellar-isochrones, stellar spectral libraries, and an IMF. Combined with a dust-law and star-formation history, SPS models create composite stellar populations (CSPs), that can be used for fitting galaxy SEDs.

As there are many different model approaches and assumptions involved, is has been largely confirmed that stellar mass are sensitive to the choice of SPS model (e.g., Wuyts et al. 2007; Cimatti et al. 2008; Muzzin et al. 2009; Longhetti & Saracco 2009; Conroy et al. 2009). In particular the different treatment of the thermally pulsating asymptotic giant branch (TP-AGB) stars between the Bruzual & Charlot (2003) and the Maraston (2005) models received a lot of attention. As the TP-AGB phase is most prominent for stellar populations around 1 Gyr, the stellar masses of galaxies at high redshift will be more affected than stellar masses at low-redshift. However, as shown by Conroy & Gunn (2010), Kriek et al. (2010), and Zibetti et al. (2013), the contribution from TP-AGB to the total light is much lower than expected from the Maraston (2005) models. Another important uncertainty comes from the SFH of a galaxy, since a large population of older stars can be hidden behind a much brighter young population. Different assumption on metallicity can further affect the stellar mass estimates. From a detailed study on a sample of massive galaxies at $z \sim 2$, Muzzin et al. (2009) find that with a maximally old stellar population superposed with a young component, the stel-

lar masses can be 0.08-0.22 dex larger as compared to exponentially declining SFHs, while different metallicities lower the stellar mass estimates by 0.10-0.16 dex.

A more fundamental uncertainty in stellar mass estimates arises from the choice of the IMF. The IMF describes the distribution of initial masses for a population of stars (e.g., Salpeter 1955; Kroupa 2002; Chabrier 2003; Kroupa et al. 2013). As stellar evolution is strongly correlated with the initial mass of a star, the IMF is an important diagnostic tool when studying large quantities of stars simultaneously. For example, with increasing initial mass, a star's mass-to-light ratio (M/L) and lifetime strongly decreases. Therefore, the integrated light of a galaxy will be dominated by the most massive stars that are still alive. Consequently, we only directly measure the mass and star-formation rate of the most massive stars still alive. The shape of IMF allows us to account for the faint low-mass stars. The IMF is therefore crucial for an accurate estimate of the total stellar mass (e.g., Courteau et al. 2013) and total star formation rate (e.g., Madau & Dickinson 2014).

The most straightforward technique to measure the IMF is counting individual stars in our Galaxy (e.g., Salpeter 1955; Kroupa 2001; Chabrier 2003). Measurements of the IMF in other galaxies are based on the integrated light of the entire stellar population. From high-S/N spectroscopic studies of nearby massive galaxies, several studies constrained the low-mass end of the IMF, either from gravity-sensitive stellar absorption features (van Dokkum et al. 2010; Spiniello et al. 2012; Smith et al. 2012; van Dokkum & Conroy 2012; Ferreras et al. 2013), or from independent mass measurements such as detailed stellar dynamics (Dutton et al. 2012; Cappellari et al. 2012, 2013), and gravitational lensing (Grillo et al. 2009; Auger et al. 2010; Treu et al. 2010; Thomas et al. 2011; Spiniello et al. 2011). In the disk of the Milky Way, the IMF is well described by a power-law $dN/dM \propto M^{-\alpha}$, with a slope of $\alpha = 2.35$ for $m > 1M_{\odot}$ (Salpeter, 1955), while below this mass, the form of the IMF is lognormal (Chabrier, 2003). The IMF may slightly vary among early-type galaxies, compared to the Milky Way. The data favor that the slope of the IMF steepens with increasing velocity, such that the cores of the most massive elliptical galaxies have a "bottom-heavy" (Salpeter or steeper) IMF (e.g., van Dokkum & Conroy 2012; Cappellari et al. 2013; Ferreras et al. 2013), but some results remain uncertain (e.g., Smith 2014).

In conclusion, uncertainties in the stellar mass estimates due to different SPS models, SFHs and metallicity can be as large as 0.6 dex (factor $\sim$4) for bright red galaxies at $z \sim 2$ (Conroy et al., 2009) while the IMF gives rise to another 0.2 dex of uncertainty. Direct stellar kinematic mass measurements, which are not affected by these uncertainties, are needed to confirm whether the stellar masses of quiescent galaxies are accurate out to $z \sim 2$.

1.7 Thesis summary

In this Thesis we assess the stellar mass estimates at high redshift, by comparing them to dynamical mass measurements, that are derived from the effective radii and stellar velocity dispersions. We furthermore explore key relations such as the Fundamental Plane, and investigate correlations between the mass-to-light ratio and color. This thesis work is built upon high-quality spectra with full UV-NIR wavelength coverage of five massive quiescent ($> 10^{11} M_{\odot}$) galaxies at $z \sim 2$, obtained with X-Shooter on the VLT. We combine these spectra with HST and ground-based multi-band photometry. Our sample is furthermore complemented with

different stellar kinematic studies from the literature at $z \sim 2$ to $z \sim 0$.

In **Chapter 2** we perform a pilot study by deriving the dynamical mass of a massive quiescent galaxy at $z = 1.8$. From the spectrum we determine a velocity dispersion of 294±51 km s^{-1}, and combine it with a size derived from HST-WFC3 image in order to derive a dynamical mass. We find that the dynamical and photometric stellar mass are in good agreement. Furthermore, the velocity dispersion at a fixed dynamical mass is a factor of ∼1.8 higher at $z = 1.8$ compared to $z = 0$. This results suggests that stellar masses at high redshift are robust, and thus supports the claim that massive, quiescent galaxies with high stellar mass densities at exist at $z \sim 2$.

Using our full sample, in **Chapter 3** we study the structural evolution of massive quiescent galaxies from $z \sim 2$ to the present-day. We measure high stellar velocity dispersions (290-450 km s^{-1}) from the spectra, and small sizes, from the HST-WFC3 H_{160} and UKIDSS-UDS K-band images. The derived dynamical masses for these galaxies show that they are very massive ($11.2 < \log M_{\rm dyn}/{\rm M}_{\odot} < 11.8$). At all redshifts, stellar and dynamical masses are tightly correlated and dynamical mass, which includes baryonic and dark matter, is always higher than stellar mass. Thus, we infer that the stellar masses are broadly correct, and that the apparent size evolution of massive galaxies in photometric studies cannot be explained by errors in the photometric masses. We confirm that at fixed mass, the effective radius increases, and the velocity dispersion decreases with time. The mass density within one effective radius decreases by more than an order of magnitude, while within 1 kpc it decreases only mildly. This finding suggests that massive quiescent galaxies at $z \sim 2$ grow in an inside-out matter, consistent with the expectations from minor mergers.

We explore the existence of a Fundamental Plane of massive quiescent galaxies at high redshift in **Chapter 4**, with the aim of measuring the evolution of the M/L from $z \sim 2$ to the present-day. We find a strong evolution of the zero point from $z \sim 2$ to $z \sim 0$: $\Delta \log_{10} M/L_{\rm g} \propto (-0.49 \pm 0.03)\, z$. However, at $z > 1$ we find that the spectroscopic sample is bluer in rest-frame $g - z$ colors, as compared to a larger mass complete sample of quiescent galaxies. We use the color offsets to estimate a M/L correction. We find that the implied FP zero point evolution after correction is significantly smaller: $\Delta \log_{10} M/L_{\rm g} \propto (-0.39 \pm 0.02)\, z$. This is consistent with an apparent formation redshift of $z_{\rm form} = 6.62^{+3.19}_{-1.44}$ for the underlying population, ignoring the effects of progenitor bias.

In **Chapter 5** we explore the dynamical mass-to-light (M/L) ratio and rest-frame colors of massive quiescent galaxies out to $z \sim 2$. Our galaxy sample spans a large range in M/L ratios: 1.8 dex in rest-frame $\log M/L_{\rm u}$, 1.6 dex in $\log M/L_{\rm g}$, and 1.2 dex in $\log M/L_{\rm K}$. We find that there is a strong correlation between the M/L ratio for different bands and rest-frame colors, that is well approximated by a linear relation. We find that it is possible to estimate the M/L of an early-type galaxy with an accuracy of ~ 0.26 dex from a single rest-frame optical color. Next, we compare the measured M/L vs. rest-frame color with different SPS models. With a Salpeter IMF, none of the SPS models are able to simultaneously match the optical and infrared colors and M/L. We test whether a different slope of the IMF provides a better match to the data. However, our results show that variations between different SPS models (with the same IMF) are comparable to the IMF variations. More complete and higher resolution empirical stellar libraries, improved stellar evolution models, and larger spectroscopic samples at high redshift, are need to provide more accurate constraints on the IMF.

References

Auger, M. W., Treu, T., Gavazzi, R., et al. 2010, ApJ, 721, L163
Bédorf, J., & Portegies Zwart, S. 2013, MNRAS, 431, 767
Bell, E. F., Naab, T., McIntosh, D. H., et al. 2006a, ApJ, 640, 241
Bell, E. F., Phleps, S., Somerville, R. S., et al. 2006b, ApJ, 652, 270
Bennett, C. L., Larson, D., Weiland, J. L., et al. 2013, ApJS, 208, 20
Bernardi, M., Sheth, R. K., Annis, J., et al. 2003, AJ, 125, 1866
Bezanson, R., van Dokkum, P. G., Tal, T., Marchesini, D., Kriek, M., Franx, M., & Coppi, P. 2009, ApJ, 697, 1290
Blanton, M. R., Eisenstein, D., Hogg, D. W., Schlegel, D. J., & Brinkmann, J. 2005, ApJ, 629, 143
Bluck, A. F. L., Conselice, C. J., Bouwens, R. J., et al. 2009, MNRAS, 394, L51
Brammer, G. B., van Dokkum, P. G., & Coppi, P. 2008, ApJ, 686, 1503
Bruzual, G., & Charlot, S. 2003, MNRAS, 344, 1000
Buitrago, F., Trujillo, I., Conselice, C. J., et al. 2008, ApJ, 687, L61
Bradač, M., Clowe, D., Gonzalez, A. H., et al. 2006, ApJ, 652, 937
Bundy, K., Fukugita, M., Ellis, R. S., et al. 2009, ApJ, 697, 1369
Cappellari, M., Scott, N., Alatalo, K., et al. 2013, MNRAS, 432, 1709
Cappellari, M., McDermid, R. M., Alatalo, K., et al. 2012, Nature, 484, 485
Cassata, P., Giavalisco, M., Guo, Y., et al. 2010, ApJ, 714, L79
Cenarro, A. J., & Trujillo, I. 2009, ApJ, 696, L43
Chabrier, G. 2003, PASP, 115, 763
Cimatti, A., Cassata, P., Pozzetti, L., et al. 2008, A&A, 482, 21
Cimatti, A., Nipoti, C., & Cassata, P. 2012, MNRAS, 422, L62
Cole, S., Lacey, C. G., Baugh, C. M., & Frenk, C. S. 2000, MNRAS, 319, 168
Clowe, D., Bradač, M., Gonzalez, A. H., et al. 2006, ApJ, 648, L109
Conroy, C., & Gunn, J. E. 2010, ApJ, 712, 833
Conroy, C., Gunn, J. E., & White, M. 2009, ApJ, 699, 486
Courteau, S., Cappellari, M., de Jong, R. S., et al. 2013, arXiv:1309.3276
Daddi, E., Renzini, A., Pirzkal, N., et al. 2005, ApJ, 626, 680
Damjanov, I., McCarthy, P. J., Abraham, R. G., et al. 2009, ApJ, 695, 101
De Lucia, G., & Blaizot, J. 2007, MNRAS, 375, 2
De Lucia, G., Springel, V., White, S. D. M., Croton, D., & Kauffmann, G. 2006, MNRAS, 366, 499
Dekel, A., Sari, R., & Ceverino, D. 2009, ApJ, 703, 785
de Ravel, L., Le Fèvre, O., Tresse, L., et al. 2009, A&A, 498, 379
di Serego Alighieri, S., Vernet, J., Cimatti, A., et al. 2005, A&A, 442, 125
Djorgovski, S., & Davis, M. 1987, ApJ, 313, 59
Dressler, A., Faber, S. M., Burstein, D., et al. 1987, ApJ, 313, L37
Dutton, A. A., Mendel, J. T., & Simard, L. 2012, MNRAS, 422, L33
Faber, S. M., & Jackson, R. E. 1976, ApJ, 204, 668
Ferreras, I., La Barbera, F., de la Rosa, I. G., et al. 2013, MNRAS, 429, L15
Feldmann, R., Carollo, C. M., Mayer, L., et al. 2010, ApJ, 709, 218
Ferré-Mateu, A., Vazdekis, A., Trujillo, I., et al. 2012, MNRAS, 423, 632
Franx, M., van Dokkum, P. G., Schreiber, N. M. F., et al. 2008, ApJ, 688, 770
Franx, M., Labbé, I., Rudnick, G., et al. 2003, ApJ, 587, L79
Grillo, C., Gobat, R., Lombardi, M., & Rosati, P. 2009, A&A, 501, 461
Guo, Q., & White, S. D. M. 2008, MNRAS, 384, 2
Herschel, W. 1786, Royal Society of London Philosophical Transactions Series I, 76, 457
Hilz, M., Naab, T., & Ostriker, J. P. 2013, MNRAS, 429, 2924
Hopkins, P. F., Hernquist, L., Cox, T. J., Keres, D., & Wuyts, S. 2009a, ApJ, 691, 1424
Hopkins, P. F., Bundy, K., Murray, N., et al. 2009b, MNRAS, 398, 898
Hopkins, P. F., Bundy, K., Croton, D., et al. 2010, ApJ, 715, 202
Hu, W., & White, M. 1996, ApJ, 471, 30
Hubble, E. 1936, Science, 84, 509
Jogee, S., Miller, S. H., Penner, K., et al. 2009, ApJ, 697, 1971
Joung, M. R., Cen, R., & Bryan, G. L. 2009, ApJ, 692, L1
Kauffmann, G., Heckman, T. M., White, S. D. M., et al. 2003, MNRAS, 341, 33

Kauffmann, G. 1996, MNRAS, 281, 487
Kauffmann, G., Charlot, S., & White, S. D. M. 1996, MNRAS, 283, L117
Kereš, D., Katz, N., Fardal, M., Davé, R., & Weinberg, D. H. 2009, MNRAS, 395, 160
Kereš, D., Katz, N., Weinberg, D. H., & Davé, R. 2005, MNRAS, 363, 2
Khochfar, S., & Silk, J. 2006, ApJ, 648, L21
Kormendy, J., Fisher, D. B., Cornell, M. E., & Bender, R. 2009, ApJS, 182, 216
Kriek, M., Labbé, I., Conroy, C., et al. 2010, ApJ, 722, L64
Kriek, M., van Dokkum, P. G., Franx, M., Illingworth, G. D., & Magee, D. K. 2009, ApJ, 705, L71
Kriek, M., van Dokkum, P. G., Labbé, I., et al. 2009b, ApJ, 700, 221
Kriek, M., van der Wel, A., van Dokkum, P. G., Franx, M., & Illingworth, G. D. 2008, ApJ, 682, 896
Kriek, M., van Dokkum, P. G., Franx, M., et al. 2006, ApJ, 649, L71
Kroupa, P., Weidner, C., Pflamm-Altenburg, J., et al. 2013, Planets, Stars and Stellar Systems. Volume 5: Galactic Structure and Stellar Populations, 115
Kroupa, P. 2002, Science, 295, 82
Kroupa, P. 2001, MNRAS, 322, 231
Labbé, I., Franx, M., Rudnick, G., et al. 2003, AJ, 125, 1107
Labbé, I., Huang, J., Franx, M., et al. 2005, ApJ, 624, L81
Longhetti, M., & Saracco, P. 2009, MNRAS, 394, 774
Longhetti, M., Saracco, P., Severgnini, P., et al. 2007, MNRAS, 374, 614
Lotz, J. M., Davis, M., Faber, S. M., et al. 2008, ApJ, 672, 177
Madau, P., & Dickinson, M. 2014, arXiv:1403.0007
Man, A. W. S., Toft, S., Zirm, A. W., Wuyts, S., & van der Wel, A. 2012, ApJ, 744, 85
Maraston, C., Daddi, E., Renzini, A., et al. 2006, ApJ, 652, 85
Maraston, C. 2005, MNRAS, 362, 799
Messier, C. 1781, Connoissance des Temps for 1784, p. 227-267, 227
Muzzin, A., Marchesini, D., Stefanon, M., et al. 2013b, ApJ, 777, 18
Muzzin, A., Marchesini, D., Stefanon, M., et al. 2013a, ApJS, 206, 8
Muzzin, A., Marchesini, D., van Dokkum, P. G., et al. 2009, ApJ, 701, 1839
Naab, T., Johansson, P. H., & Ostriker, J. P. 2009, ApJ, 699, L178
Naab, T., Johansson, P. H., Ostriker, J. P., & Efstathiou, G. 2007, ApJ, 658, 710
Nipoti, C., Treu, T., Leauthaud, A., et al. 2012, MNRAS, 422, 1714
Nipoti, C., Treu, T., Auger, M. W., & Bolton, A. S. 2009, ApJ, 706, L86
Newman, A. B., Ellis, R. S., Bundy, K., & Treu, T. 2012, ApJ, 746, 162
Onodera, M., Renzini, A., Carollo, M., et al. 2012, ApJ, 755, 26
Oogi, T. & Habe, A. 2012, MNRAS, 42
Oser, L., Naab, T., Ostriker, J. P., & Johansson, P. H. 2012, ApJ, 744, 63
Oser, L., Ostriker, J. P., Naab, T., Johansson, P. H., & Burkert, A. 2010, ApJ, 725, 2312
Papovich, C., Dickinson, M., Giavalisco, M., Conselice, C. J., & Ferguson, H. C. 2005, ApJ, 631, 101
Perlmutter, S., Aldering, G., Goldhaber, G., et al. 1999, ApJ, 517, 565
Riess, A. G., Filippenko, A. V., Challis, P., et al. 1998, AJ, 116, 1009
Salpeter, E. E. 1955, ApJ, 121, 161
Saracco, P., Gargiulo, A., & Longhetti, M. 2012, MNRAS, 422, 3107
Schawinski, K., Urry, C. M., Simmons, B. D., et al. 2014, MNRAS, 440, 889
Shen, S., Mo, H. J., White, S. D. M., et al. 2003, MNRAS, 343, 978
Slipher, V. M. 1918, Publications of the American Astronomical Society, 3, 98
Smith, R. J. 2014, arXiv:1403.6114
Smith, R. J., Lucey, J. R., & Carter, D. 2012, MNRAS, 426, 2994
Spiniello, C., Trager, S. C., Koopmans, L. V. E., & Chen, Y. P. 2012, ApJ, 753, L32
Spiniello, C., Koopmans, L. V. E., Trager, S. C., Czoske, O., & Treu, T. 2011, MNRAS, 417, 3000
Steidel, C. C., Giavalisco, M., Dickinson, M., & Adelberger, K. L. 1996a, AJ, 112, 352
Steidel, C. C., Giavalisco, M., Pettini, M., Dickinson, M., & Adelberger, K. L. 1996b, ApJ, 462, L17
Straatman, C. M. S., Labbé, I., Spitler, L. R., et al. 2014, ApJ, 783, L14
Szomoru, D., Franx, M., van Dokkum, P. G., et al. 2013, ApJ, 763, 73
Szomoru, D., Franx, M., & van Dokkum, P. G. 2012, ApJ, 749, 121
Szomoru, D., Franx, M., Bouwens, R. J., et al. 2011, ApJ, 735, L22
Szomoru, D., Franx, M., van Dokkum, P. G., et al. 2010, ApJ, 714, L244

Taylor, E. N., Franx, M., Glazebrook, K., et al. 2010, ApJ, 720, 723
Thomas, J., Saglia, R. P., Bender, R., et al. 2011, MNRAS, 415, 545
Toft, S., van Dokkum, P., Franx, M., et al. 2007, ApJ, 671, 285
Tran, K.-V. H., van Dokkum, P., Franx, M., et al. 2005, ApJ, 627, L25
Treu, T., Auger, M. W., Koopmans, L. V. E., et al. 2010, ApJ, 709, 1195
Trujillo, I., Cenarro, A. J., de Lorenzo-Cáceres, A., et al. 2009, ApJ, 692, L118
Trujillo, I., Förster Schreiber, N. M., Rudnick, G., et al. 2006, ApJ, 650, 18
Tully, R. B., & Fisher, J. R. 1977, A&A, 54, 661
van der Wel, A., Franx, M., van Dokkum, P. G., et al. 2014, ApJ, 788, 28
van der Wel, A., Holden, B. P., Zirm, A. W., et al. 2008, ApJ, 688, 48
van der Wel, A., Franx, M., van Dokkum, P. G., et al. 2005, ApJ, 631, 145
van Dokkum, P. G., & Conroy, C. 2012, ApJ, 760, 70
van Dokkum, P. G., et al. 2010, ApJ, 709, 1018
van Dokkum, P. G., et al. 2008, ApJ, 677, L5
van Dokkum, P. G. 2005, AJ, 130, 2647
van Dokkum, P. G., Förster Schreiber, N. M., Franx, M., et al. 2003, ApJ, 587, L83
Whitaker, K. E., Labbé, I., van Dokkum, P. G., et al. 2011, ApJ, 735, 86
Whitaker, K. E., Kriek, M., van Dokkum, P. G., et al. 2012, ApJ, 745, 179
Williams, R. J., Quadri, R. F., Franx, M., van Dokkum, P., & Labbé, I. 2009, ApJ, 691, 1879
Wuyts, S., Labbé, I., Schreiber, N. M. F., et al. 2008, ApJ, 682, 985
Wuyts, S., Labbé, I., Franx, M., et al. 2007, ApJ, 655, 51
York, D. G., Adelman, J., Anderson, J. E., Jr., et al. 2000, AJ, 120, 1579
Zibetti, S., Gallazzi, A., Charlot, S., Pierini, D., & Pasquali, A. 2013, MNRAS, 428, 1479